II. INTERMETALLIC COMPOUNDS WITH LANTHANIDES

2.1 Crystal structures

Alloys and (ordered) compounds of lanthanides (R) and other metals (M) have been extensively studied over the past twenty years. This is reflected by Taylor's review article [7] and Wallace's book [8] on compounds of rare earths with other metals.

Since chemical properties do not vary over the range of lanthanides, except phenomena related to a change of valence in Ce, Yb and sometimes Eu, a specific compound is formed usually with all R. Moreover, a particular structure type occurs usually with more than one specific M. The most common example of this is possibly found in the AB_2 Laves phases which occur for quite a number of intermetallic systems, including RM_2 compounds. Lastly, families of structures exist that can be thought of as derived from one common basic structure. These features enable one to study metallic interactions between well-localized and more diffuse magnetic moments under widely varying, but related, conditions.

The present work is concerned with a family of compounds between on one hand Y, Th and lanthanides proper and on the other hand the 3d transition metals Fe, Co, Ni. The parent structure has the composition RM_5 and is known as the $CaCu_5$ structure. Its symmetry is hexagonal, space group P6/mmm, with atomic positions

R at 1(a) 000 with point symmetry 6/mmm

M_1 at 2(c) $\pm(\frac{1}{3},\frac{2}{3},0)$ with point symmetry $\bar{6}$ m 2

M_2 at 3(g) $0\frac{1}{2}\frac{1}{2}$, $\frac{1}{2}0\frac{1}{2}$, $\frac{1}{2}\frac{1}{2}\frac{1}{2}$, with point symmetry mmm,

in a unit cell of dimensions $a = b \simeq 5.0$ Å, $c \simeq 4.0$ Å

This structure is visualized in fig. 4.

The shortest interatomic distances are:

$$M_1 - M_2 \simeq M_2 - M_2 \simeq 2.5 \text{ Å}$$

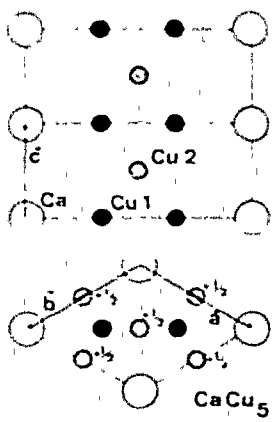

Fig. 4. The $CaCu_5$ crystal structure exhibited by RM_5 compounds. The R atom occupies the Ca site, M is found on the Cu sites. The upper part of the figure gives a *section* through the crystal perpendicular to the a-b plane; this method of presentation is adopted in all related figures. The lower part gives a *projection* on the a-b plane.

$$R - M_1 = M_1 - M_1 = 3.0\ \text{Å}$$
$$R - M_2 = 3.3\ \text{Å}$$

The atoms are arranged in two different kinds of layers separated by $\frac{1}{2}c = 2.0$ Å. One layer, at $z = 0$, consists of hexagons of M_1, the centres of which are occupied by R atoms. The other layer at $z = \frac{1}{2}$ contains the M_2 atoms arranged on what is known as a kagome net, such that the R and M_1 in adjacent layers fit in the large and small holes respectively, cf. fig. 5. Each M_2 atom has four nearest neighbours of its own kind, in addition to two M_1 and two R atoms in each adjacent layer, totalling 8M + 4R. Second nearest neighbours are other M_2 atoms.

An M_1 atom has, apart from 3 R atoms, M_2 atoms as its nearest neighbours, three in each neighbouring layer. The three M_1 in the same layer are second neighbours. The two different M sites are therefore not merely crystallographically inequivalent, but are also located in physically very different environments.

From this basic structure type one may derive other structures by systematic substitutions.

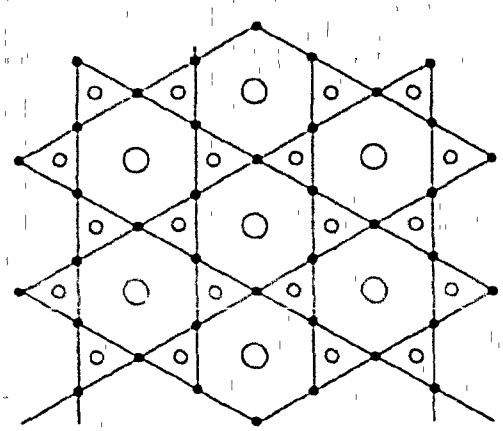

Fig. 5. Extended projection of $CaCu_5$ crystal structure. Black circles connected by solid lines give the M_2 kagome arrangement at $z = \frac{1}{2}$; large and small open circles represent Th and M_1 at $z = 0$.

The first of these substitution schemes yields an M-rich compound by the replacement of 1/3 of the R atoms by a pair of M:

$$3\ RM_5 - R + 2\ M = R_2M_{17}.$$

In addition to a truly random replacement two regular substitution schemes are realized, shown in fig. 6a, of hexagonal or rhombohedral symmetry. Many R can form both structure types. As a consequence disorder is possible in these compounds. Since this is discussed in detail in chapter VI we limit ourselves here to note that similar mechanisms might be active in other compounds forming both hexagonal and rhombohedral structures.

The other substitution schemes known lead to M-poorer compounds, all being based on the replacement of some M_1 by R. In the RM_2 compounds (fig. 6b) this is done in every RM_5 unit:

$$RM_5 - M + R = 2\ RM_2.$$

These are the Laves phases already mentioned. The M_2 atoms now have one M_1 and three R neighbours on either side, as well as the four M_2 as before; for the M_1 atoms the nearest neighbour configuration is unchanged. In RM_3 compounds (fig. 6c) the substitution is effected in every second block:

$$2\ RM_5 - M + R = 3\ RM_3.$$

The M_1 site now splits in two inequivalent sites, one of RM_5 and one of RM_2 type; the M_2 site does not split crystallographically but has an RM_5 type layer at one side and one of RM_2 type at the other side.

Finally, in R_2M_7 compounds (fig. 6d) the substitution occurs in every third block:

$$3\ RM_5 - M + R = 2\ R_2M_7.$$

Again the M_1 site is split; now also M_2 splits in one of RM_5 type and two of RM_3 type.

For the existence of phases based on a further extension of this scheme evidence is scarce [9]. This suggests an estimate of the range of interatomic forces in these crystals: beyond approximately $3 \times 4 = 12$ Å there is little, if any, correlation between substitutions, and in fact beyond 8 Å correlations appear to diminish.

Whereas the Laves phases are very common the same is not true for the other members of the family. In R-M systems they are rarely found for other M than Fe, Co or Ni, and even so not all structures are found for all possible combinations: notable absences are RFe_5 and R_2Fe_7 other than for R = Th; hexagonal RM_3 appears to be stable for M = Ni only, and RFe_2 similarly for the heavy lanthanides.

2.2 Exchange interactions

One, typically metallic, exchange mechanism is indirect coupling via itinerant electrons. The basic idea is the following: assume a localized moment at the origin in a Fermi sea; exchange between the localized ("f") and itinerant ("s") electrons polarizes the latter. In a first order perturbation calculation a uniform polarization results; in second order an oscillating polarization is found. A second localized moment at position $\vec{R}$ is sensitive to the local polarization through the same exchange interaction with the itinerant electrons, and thereby is indirectly coupled to the magnetic moment at the origin. The strength of this coupling depends quadratically on the f-s exchange constant and the itinerant electron density at the Fermi surface, but also on the magnitude and sense of the local polarization.

This theory, known as RKKY after Rudermann, Kittel, Kasuya and Yosida, was originally developed for the interpretation of NMR experiments, then extended to the use for dilute magnetic alloys and applied with some success

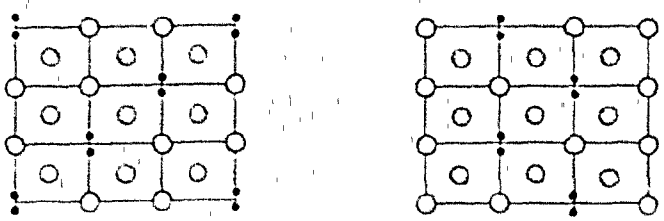

Fig. 6a. R_2M_{17}

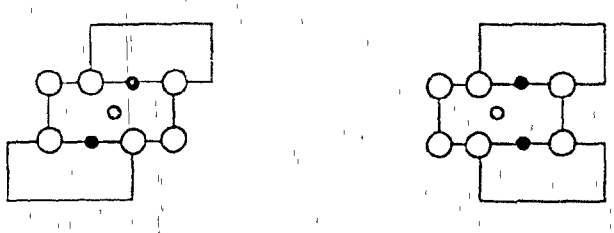

Fig. 6b. RM_2

Figs. 6a - 6d. Stacking sequence and substitution schemes.
Both hexagonal and rhombohedral stacking are shown.
6a: R_2M_{17}; 6b: RM_2; 6c: RM_3; 6d: R_2M_7.
The symbols used are those of fig. 4.

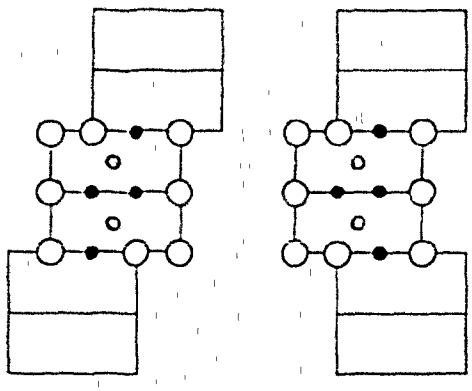

Fig. 6c, RM_3

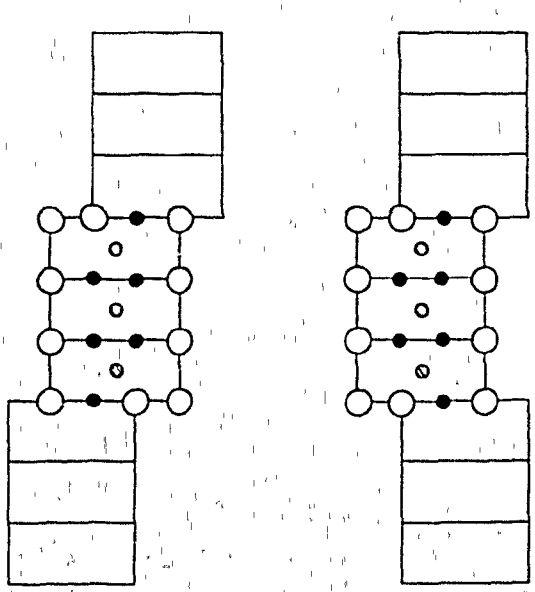

Fig. 6d, R_2M_7

to alloys and compounds between lanthanides and simple metals.

Though the basic idea is very clear an exact treatment in real cases is extremely difficult if not impossible. An exact calculation of the exchange constant V is already impossible at the moment; usually $V(\vec{R},\vec{r}) = V_o \delta(\vec{R}-\vec{r})$ is assumed, which implies a constant $V(\vec{q}) = V$ in momentum space. With the further simplification of plane wave itinerant electrons and an exactly localized moment $\vec{S}$ at the origin the resulting second order spin polarization can be calculated. The next step is the derivation of the indirect exchange hamiltonian between spins $\vec{S}_i$ at $\vec{R}_i$ and $\vec{S}_j$ at $\vec{R}_j$. This is found to be of the Heisenberg form:

$$H = \sum_{ij} H_{ij}$$

$$H_{ij} = -J(\vec{R}_{ij})\, \vec{S}_i \cdot \vec{S}_j$$

with the exchange parameter

$$J(\vec{R}_{ij}) \sim c^2 V^2 F_{ij}(2 k_f R_{ij})$$

In this expression c is the itinerant electron concentration at the Fermi surface, V the constant exchange parameter in q-space, k_f the radius of the Fermi sphere and

$$F_{ij}(x) = \frac{\sin x - x \cos x}{x^4}$$

When this theory is applied to lanthanide ions one must take into account that $\vec{S}$ is not conserved because of spin-orbit coupling and must be replaced by $(g-1)\vec{J}$ [7]; then, for a particular series of alloys with the same $\Sigma F_{ij}(x)$ molecular field treatment yields a (paramagnetic) Curie temperature

$$\theta_p \sim c^2 V^2 (g-1)^2 J(J+1) \sum_{ij} F_{ij}(2 k_f R_{ij}).$$

The proportionality between θ_p and the De Gennes function $(g-1)^2 J(J+1)$ has been shown to hold in a number of systems; however, this proves the validity of a Heisenberg type hamiltonian only unless the proper c- and F dependence of J are demonstrated as well.

Freeman [10] discusses more refined treatments of RKKY theory, including the consequences of a non-spherical Fermi surface, correlation and exchange effects, non-constant V(q) and interband mixing, but he concludes that the present state of theory and experiment is insufficient to decide on the form and magnitude of these effects. There is little doubt that

RKKY exchange is a fundamental mechanism in magnetic metals and alloys, especially for lanthanides with their well-localized 4f-shell. The situation is not so clear if the theory is to be applied to 3d-metals as s-d exchange, since the d-electrons are not strictly localized.

The theory of d-d exchange in transition metals is connected to that of the formation of localized magnetic moments and long-range magnetic order. By a shift of the spin-up band with respect to the spin-down band exchange energy can be gained but kinetic energy is lost, from which the well-known Stoner stability criterion follows (cf. textbooks on metals). This should not concern us here, since neutron form factors for metallic 3d electrons show that in fact they are essentially localized.

Friedel [11] discusses the behaviour of electrons in a d-band in tight binding approximation and shows how, in second order approximation, a mechanism similar to RKKY theory applies to d-d exchange. He proceeds to show how ferromagnetic and antiferromagnetic structures may arise as a function of d-electron concentration, Fermi radius or susceptibility. However, he also points out that for large magnetic moments perturbation theory is not applicable and that couplings between more than two moments must be taken into account.

We may draw attention to a band-structure calculation by Duff and Das for Fe [12], in which a correct value of the magnetic moment and good electron and spin densities were obtained, starting from almost first principles, using slightly diffuse 3d wave functions. It was estimated that there is about 5% admixture of itinerant behaviour in otherwise atomic d-functions. This small amount of itinerancy is thought to be essential for the establishment of ferromagnetism in Fe. Whereas this shows that a realistic band-structure calculation, incorporating localized moments, is possible for Fe, to our knowledge a similar calculation was not yet reported for Ni or Co. No band-structures at all are known for the compounds that are the subject of this thesis, so we have no information about the shape of the Fermi surface or the magnitudes of band widths and splittings.

2.3 Results obtained by other workers

Because of their high coercivity, anisotropy, induction and Curie temperature the R-Co compounds have technical importance as possible permanent magnet materials. Therefore these compounds have been thoroughly

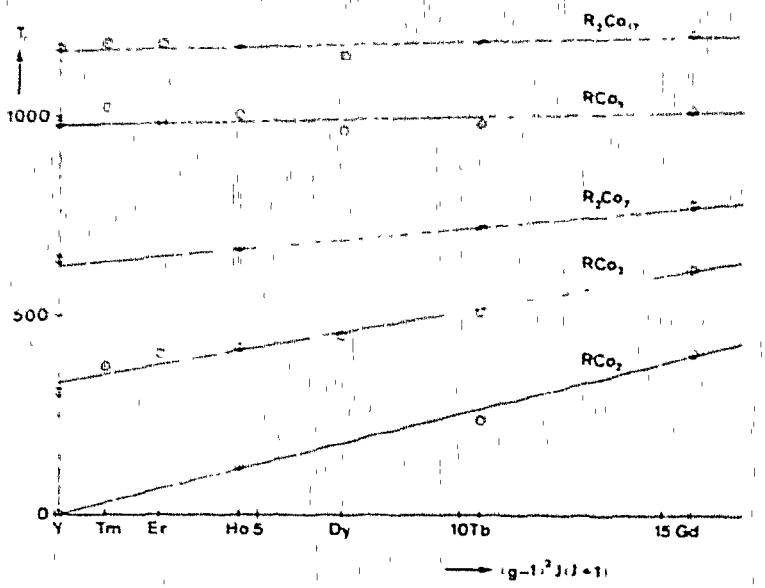

Fig. 7a Curie-temperatures as function of $(g-1)^2\,J(J+1)$ for heavy R-Co compounds.

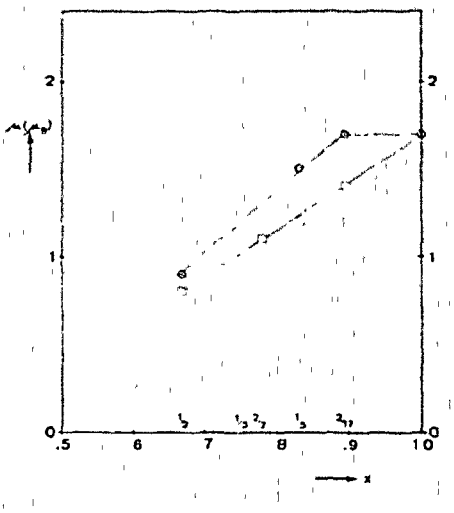

Fig. 7b Average Co-moment in $R_{1-x}Co_x$;
circles: heavy R;
squares: light R.

investigated. It has been found as a general rule that compounds with a light R, where $\vec{S}$ and $\vec{J}$ are antiparallel, are ferromagnetic and that compounds with a heavy R, with parallel $\vec{S}$ and $\vec{J}$, are ferrimagnetic ([5], [13]). This means that the spins of R and Co are always antiparallel, which is hardly compatible with RKKY theory ([8], p. 176). Crystal fields, together with an internal field due to the Co moment, determine the direction of easy magnetization [13], which usually but not always

In fig. 7a the Curie-temperatures T_c of a number of heavy-lanthanide-Co compounds are shown as a function of $(g-1)^2 J(J+1)$, the DeGennes function of the lanthanide ion. For light R there is more scatter in T_c: Pr and Nd compounds usually have a lower T_c than expected, which is probably due to crystal field effects. In fig. 7a indeed a term linear in the DeGennes function is found. It is tempting to attribute this to indirect exchange between R and Co, and to ascribe the constant term to direct and indirect exchange interaction between Co atoms.

The average magnetic moment per Co atom in RCo_x compounds is given in fig. 7b. It is seen that the moment is generally lower for light R. For RCo_3 the sublattice magnetization is not known; when one tries to split the measured moment per unit cell in a full-ion R part and the remainder as Co, highly improbable values for the Co moment result, indicating that the R moment must be reduced by crystal fields.

In figs. 8 and 9 results are presented in the same fashion for R-Ni and R-Fe compounds. These systems were not investigated as extensively as the Co-compounds. In the older literature Ni is reported to be non-magnetic, but later workers found an appreciable Ni-moment in R_2Ni_{17} compounds and a small value in RNi_2 and RNi_3. In RNi_5 no magnetic moment is found on the Ni atoms [13]. In the R-Fe system the R_2Fe_{17} compounds have been investigated. The ferro- or ferrimagnetic coupling scheme found for Co compounds is valid for R_2Fe_{17} compounds as well. Their anisotropy is usually planar, with the exception of Tm_2Fe_{17} below 72 K (Cf. VI, 6.2). A very interesting feature of the R_2Fe_{17} compounds with non-magnetic R is the occurrence of helical magnetic order [15], [21]. This is thought to originate in an antiferromagnetic exchange interaction among the substituted Fe (cf. fig. 6a) which have very short nearest neighbour distances (< 2.5 Å). As soon as a magnetic moment develops on the R site the helical configuration is disturbed and the structure becomes collinear.

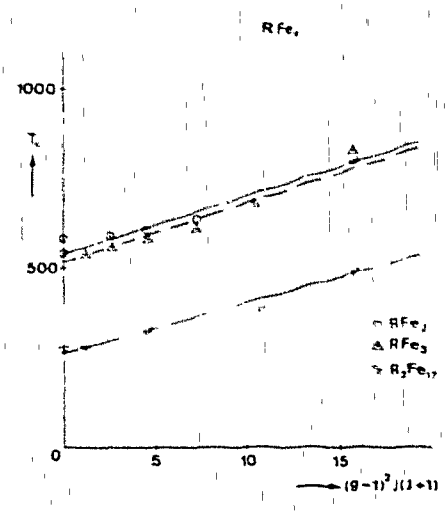

Fig. 8a Curie temperatures as function of $(g-1)^2\ J(J+1)$ for heavy R-Fe compounds.

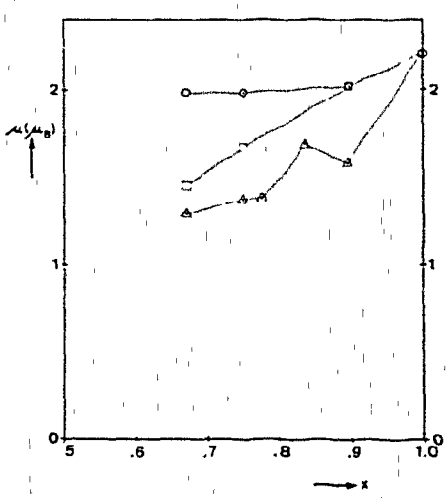

Fig. 8b Average moment in $R_{1-x}Fe_x$.
circles: heavy R;
squares: light R.
triangles: Th.

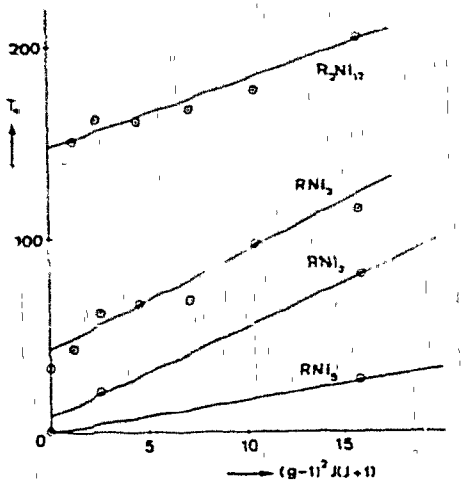

Fig. 9. Curie temperatures as function of $(g-1)^2\ J(J+1)$ for heavy R-Ni compounds.

2.4 The scope of the present investigation

So far only lanthanides proper and Y, which behaves as a non-magnetic heavy R, have been mentioned. Since the conduction electron concentration is one of the parameters involved it is a natural extension to investigate Th compounds as well, since Th also behaves as a non-magnetic heavy R but contributes four conduction electrons to the Fermi sea. In table I a survey is given of the known compounds of Th with Fe, Co and Ni that are derived from the $CaCu_5$ structure.

The diffraction experiments described encompass all compounds that show long-range magnetic order. The work started with an investigation of the pseudo-binary system $Th(Co, Fe)_5$ in order to facilitate the interpretation of Mössbauer experiments on these compounds. The results stimulated a further investigation of magnetic order in compounds between Th and Fe, Co, N

This first analysis of $Th(Co,Fe)_5$ is reported in chapter III; in chapters IV and V the results obtained for $Th(Ni,Fe)_5$ and $Th(Co,Ni)_5$ are given.

Table 1. Compounds of Th with Fe, Co or Ni, derived from the Cu-Mn structure.

compounds with Fe

	Symmetry	T_c (K)	μ/atom
$ThFe_3$	$R\bar{3}m$	~25	1.37
α-Th_2Fe_7	$P6_3/mmc$	570	1.37
$ThFe_5$	$P6/mmm$	680	1.88
Th_2Fe_{17}	$R\bar{3}m$	295	1.76

compounds with Co

Th_2Co_7	$P6_3/mmc$	paramagnetic	
$ThCo_5$	$P6/mmm$	415	0.94
Th_2Co_{17}	$R\bar{3}m$	1035	1.42

compounds with Ni

$ThNi_5$	$P6/mmm$	paramagnetic
Th_2Ni_{17}	$P6_3/mmc$	paramagnetic

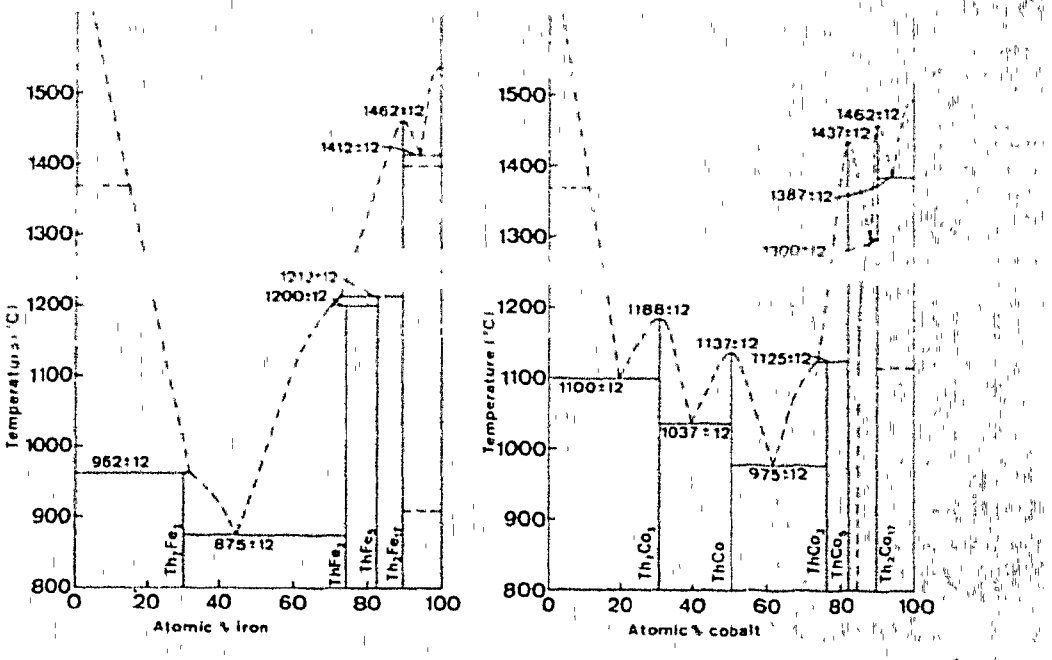

Fig. 10. Phase diagrams of $Th_{100-x} - Fe_x$ and $Th_{100-x} - Co_x$ (right) taken from ref. 16, cf. text for later revisions.

R_2M_{17} compounds are the subject matter of chapter VI. It is not limited to Th-compounds but has a more general stand point, discussing disorder in hexagonal R_2M_{17} compounds and supporting the discussion with experimental evidence.

Th_2Fe_{17} and Th_2Co_{17} are plain ferromagnets with planar anisotropy; no further discussion will be given of the diffraction experiment on these two compounds since the analysis was straight-forward and yielded immediate results.

Magnetic order in $ThFe_3$ and Th_2Fe_7 will be discussed in chapter VII.

Finally, chapter VIII is devoted to a critical evaluation of the results in relation to other experiments.

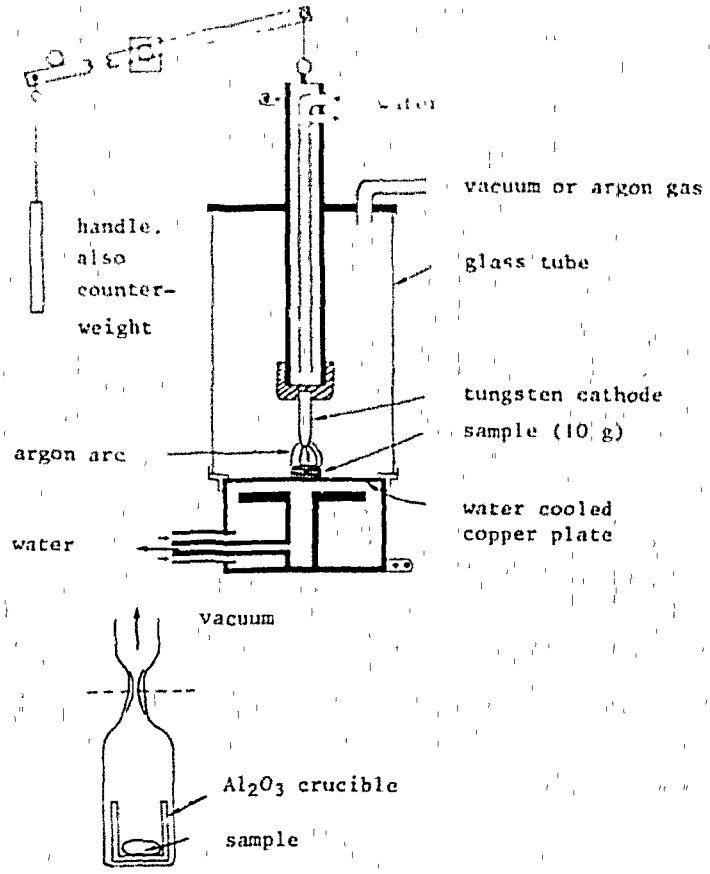

Fig. 11. Arc-melting apparatus and annealing configuration (courtesy of K.H.J. Buschow).

2.5 The samples

In the papers reproduced in chapters III through VII there is no particular emphasis on sample preparation. Therefore this chapter is concluded with a more detailed description of the procedure followed. The information in this section is made available through the courtesy of K.H.J. Buschow.

Phase diagrams for Th-Fe and Th-Co systems were reported in 1966 [16] and they are reproduced in fig. 10. In later years the compound Th_2Fe_7 was discovered. Moreover, $ThFe_5$ was found to be unstable below T = 1000 ^{o}C [17].

A drawing of the equipment used in sample preparation is presented in fig. 11. The procedure is as follows:

The proper amounts of the constituent elements are placed on the copper plate in the arc-melting apparatus, after which the equipment is evacuated and filled with purified Ar gas to a pressure of 10-20 cm Hg. An electric arc is lit between the tungsten cathode and the metal pieces lying on the water-cooled copper plate. In order to ensure chemical homogeneity the button is turned over and remelted about four times. After the melting process the button is annealed, particularly if the compound has a peritectic melting point, in order to remove phases adjacent in the phase diagram. The alloy button is placed in a sintered Al_2O_3 crucible which in turn is sealed in a silica tube. The tube is evacuated for one or two hours whilst gently heated in order to remove all traces of adsorbed oxygen or water vapour, and then sealed. The sealed tube is placed in a resistance furnace and kept at the temperature during the time as indicated in the experimental section in each chapter.